CHEMISTRY
A EUROPEAN JOURNAL

DOI: 10.1002/chem.201001084

Control of the Optical Properties of a Star Copolymer with a Hyperbranched Conjugated Polymer Core and Poly(ethylene glycol) Arms by Self-Assembly

Feng Qiu,[a] Chunlai Tu,[a] Yan Chen,[a] Yunfeng Shi,[a] Liang Song,[a] Ruibing Wang,[b] Xinyuan Zhu,*[a, b] Bangshang Zhu,*[b] Deyue Yan,[a] and Tao Han*[c]

Abstract: A self-assembly approach to tuning the optical properties of a star copolymer is reported herein. The star copolymer HCP-*star*-PEG with a hyperbranched conjugated polymer (HCP) core and many linear poly(ethylene glycol) (PEG) arms has been prepared successfully. The HCP core was synthesized by Wittig coupling of *N*-(*n*-hexyl)-3,6-diformylcarbazole and 1,3,5-bis[(triphenylphosphonio)methyl]-benzene tribromide. Subsequently, the linear PEG arms were grafted onto the HCP core by acylhydrazone connection. It was found that the optical properties of HCP-*star*-PEG in chloroform solution changed on addition of acid. Both ^{1}H NMR and UV/Vis spectroscopic investigations confirmed that the variation of the optical properties was related to the complexation of the acid and the imine bond in the acylhydrazone group. HCP-*star*-PEG self-assembled into core–shell micelles in the mixed solvent of chloroform and acetonitrile, which affected the protonation of the imine bond. Therefore the optical properties of HCP-*star*-PEG can be readily controlled by self-assembly.

Keywords: micelles · optical properties · polymers · polymerization · self-assembly

Introduction

Supramolecular self-assembly based on non-covalent interactions has attracted increasing attention.[1] Owing to their unique optoelectronic properties, for example, emission efficiency, charge transfer, and energy transfer, the self-assembly of π-conjugated systems has been investigated intensively.[2] To date, various morphologies, including micelles, cylinders, fibers, and films, have been obtained from small conjugated molecules,[2c,3] conjugated dendrimers,[4] and rod–coil block conjugated polymers.[5] Among them, linear rod–coil block conjugated polymers are particular interesting because both the assembled morphology and related optoelectronic properties can be readily adjusted by the molecular weight, composition, configuration, conformation, and architecture.[6]

For linear rod–coil block conjugated polymers, the optoelectronic properties can be improved by changing their aggregation behavior (H- or J-aggregates).[7] In the solid state, the electroluminescent properties can also be enhanced by the evolution of the phase structure.[5b] Unfortunately, nonradiative decay occurs in the supramolecular self-assembly of linear rod–coil block conjugated copolymers as a result of interchain electronic interactions of rigid segments through π–π stacking.[5d,e,i] To weaken the strong π–π interactions, a highly branched architecture has been introduced into the conjugated polymer systems to avoid regular molecular stacking.[8] However, to the best of our knowledge, the preparation and self-assembly of a star copolymer with a hyperbranched conjugated polymer core have rarely been reported. More importantly, the influence of self-assembly behav-

[a] F. Qiu, C. Tu, Y. Chen, Y. Shi, L. Song, Prof. X. Zhu, Prof. D. Yan
School of Chemistry and Chemical Engineering
State Key Laboratory of Metal Matrix Composites
Shanghai Jiao Tong University
800 Dongchuan Road, Shanghai 200240 (P.R. China)
Fax: (+86) 21-3420-5722
E-mail: xyzhu@sjtu.edu.cn

[b] R. Wang, Prof. X. Zhu, Prof. B. Zhu
Instrumental Analysis Center
Shanghai Jiao Tong University
800 Dongchuan Road, Shanghai 200240 (P.R. China)
Fax: (+86) 2134205722
E-mail: xyzhu@sjtu.edu.cn
bshzhu@sjtu.edu.cn

[c] Prof. T. Han
Department of Instrument Science and Engineering, Shanghai Jiao Tong University
800 Dongchuan Road, Shanghai 200240 (P.R. China)
Fax: (+86) 2134205372
E-mail: than@sjtu.edu.cn

Supporting information for this article is available on the WWW under http://dx.doi.org/10.1002/chem.201001084.

ior on the optoelectronic properties of such a star copolymer has not yet been studied.

In this work a novel star copolymer (HCP-*star*-PEG) with acylhydrazone linkers between a hyperbranched conjugated polymer (HCP) core and many linear poly(ethylene glycol) (PEG) arms was synthesized. As a result of the existence of the imine bond (C=N) in the acylhydrazone group, HCP-*star*-PEG in chloroform solution showed clear optical change after protonation or complexation with metal ions. On addition of acetonitrile, HCP-*star*-PEG self-assembled into nanoparticles, which affected the protonation of the imine group greatly. Therefore the optical properties of HCP-*star*-PEG can be controlled successfully through self-assembly.

Results and Discussion

Synthesis and characterization: The synthetic route to the novel hyperbranched conjugated polymer (HCP) and star copolymer (HCP-*star*-PEG) is shown in Scheme 1. The hyperbranched conjugated polymer (HCP, 7) was formed from monomers **2** and **4** through an A_2+B_3-type Wittig coupling reaction. Owing to the fast initialization and slow propagation of the polymerization reaction, the molecular weight and terminal functional group were easy to control in this synthesis.[9] For example, when the molar ratio of A_2 to B_3 was 2:1, the terminal functional group of HCP was the aldehyde. The proton signals at $\delta = 10$ and 5.00 ppm in Figure 1a and b are assigned to the C*H*O proton of monomer **2** and

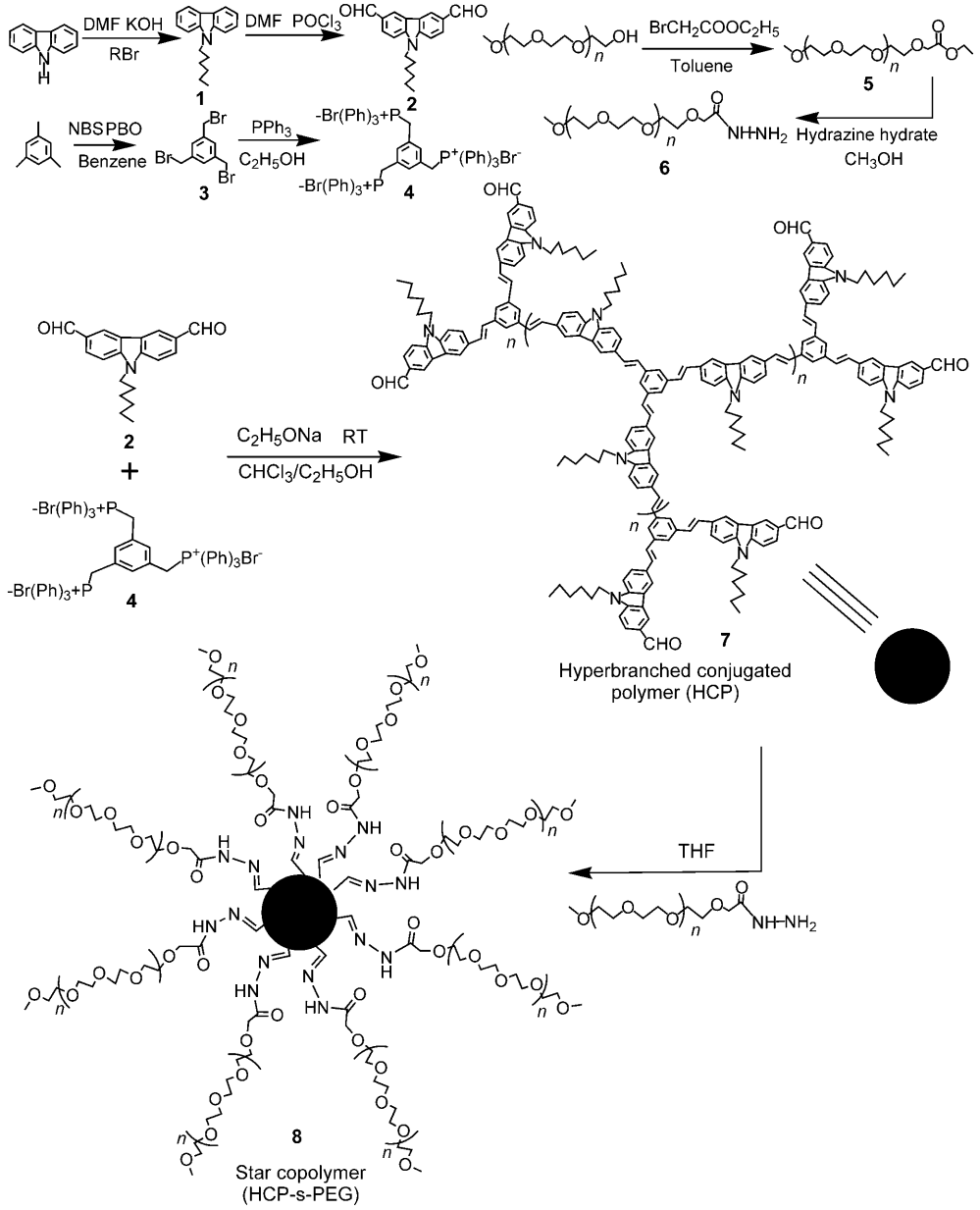

Scheme 1. Synthetic route to the monomers, HCP, and HCP-*star*-PEG.

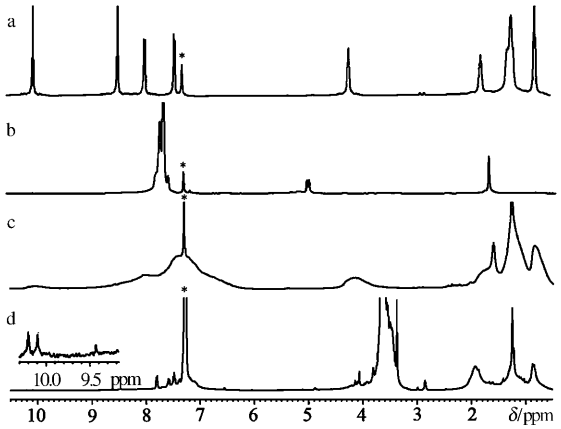

Figure 1. ^{1}H NMR spectra of a) the A_2 monomer **2**, b) the B_3 monomer **4**, c) HCP **7** ($A_2/B_3=2:1$), and d) HCP-*star*-PEG **8** (400 MHz, $CDCl_3$, 20 °C; the solvent peak is marked with asterisk).

the CH_2Br protons of monomer **4**, respectively. For HCP, Figure 1c shows that the former still exists whereas the latter disappears.

The degree of branching (DB) is an important topological parameter for hyperbranched polymers and is often determined by NMR spectral analysis.[10] Generally speaking, the DB of a hyperbranched conjugated polymer is difficult to determine because the individual aromatic signals severely overlap in a very narrow range. Fortunately, the DB of our HCP can be calculated when it is dissolved in deuteriated dichloromethane; the DB of HCP was found to be about 0.77, which is higher than the values of "conventional" hyperbranched polymers ($DB \leq 0.5$). (Details of the calculation of DB are given in the Supporting Information.) Hyperbranched conjugated polymers with high values of DB have also been reported in the literature.[8e,f,11] In our system, the high DB is probably related to the efficient Wittig coupling reaction between the aldehyde group and the triphenylphosphoniomethyl bromide.

HCP reacted with poly(ethylene glycol) monomethyl ether with an acylhydrazine terminal (**6**) to give the star copolymer HCP-*star*-PEG (**8**) with an acylhydrazone linker. The peaks at $\delta = 9.4$ and 10.2 ppm in the ^{1}H NMR spectrum of HCP-*star*-PEG (Figure 1d) are attributed to the protons of C*H*=N and N*H*–CO in the acylhydrazone bond. In addition, a strong OCH_2CH_2O signal at $\delta = 3.65$ ppm was observed, which further confirms the grafting of the PEG arms onto the HCP. Based on the ^{1}H NMR spectrum of Figure 1d, the grafting ratio (g) of HCP-*star*-PEG was determined to be 0.91. Details are given in the Supporting Information.

The FTIR spectra of monomers **2** and **4**, HCP and HCP-*star*-PEG are given in Figure 2. Figure 2a exhibits a strong absorption band at 1681 cm^{-1} associated with the stretching of the aldehyde group of monomer **2**. In the FTIR spectrum of monomer **4** (Figure 2b), an absorption band at 509 cm^{-1} ascribed to the C–Br stretching vibration is observed. For HCP, only the absorption band of the aldehyde group is observed in Figure 2c, which indicates the complete reaction of

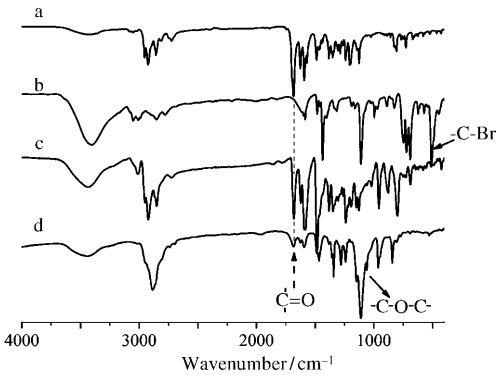

Figure 2. The FTIR spectra of a) monomer **2**, b) monomer **4**, c) HCP, and d) HCP-*star*-PEG.

the triphenylphosphoniomethyl bromide during the polymerization. This result is consistent with the ^{1}H NMR analysis. The spectral profile of HCP seems to be a superposition of those of monomers **2** and **4**, except for the weakening of aldehyde absorption and the disappearance of the C–Br stretching vibration. This suggests that only the aldehyde and triphenylphosphoniomethyl bromide react during the polymerization and the resulting polymer shares the basic molecular structure of the two monomers. When the PEG arms are grafted onto the HCP, the aldehyde absorption is weakened greatly with the appearance of a very strong C–O–C stretching band at 1112 cm^{-1} arising from the PEG, as shown in Figure 2d.

Molecular weight, stability, and solubility: The number- and weight-average molecular weights (M_n and M_w), M_w/M_n, and thermal properties of HCP and HCP-*star*-PEG are summarized in Table 1. The decomposition temperature of HCP

Table 1. Molecular weights, polydispersities, and thermal data for HCP and HCP-*star*-PEG.

	M_w (10^4)	M_n (10^4)	M_w/M_n	dn/dc[a]	T_d[b] [°C]	W[c] [%]
HCP	0.40	0.77	2.0	0.20	428	45.0
HCP-*star*-PEG	2.60	3.65	1.4	0.08	367	9.4

[a] Refractive index increment. [b] The temperature at 5% weight lost. [c] The residual weight at 800 °C.

with 5% weight loss ($T_{d-5\%}$) is 428 °C. Due to the presence of many PEG arms, the decomposition temperature of HCP-*star*-PEG with 5% weight loss ($T_{d-5\%}$) decreases to 367 °C. This indicates that both HCP and HCP-*star*-PEG have excellent thermal stability. In addition, the polymers are soluble in common organic solvents like THF, toluene, and chloroform, which indicates good solution processability for some applications.

Optical properties of HCP-*star*-PEG: The optical properties of HCP-*star*-PEG in chloroform were investigated. Figure 3a shows that the UV/Vis absorption peaks of HCP-*star*-PEG are located at 250–420 nm. The absorption peaks at 256 and

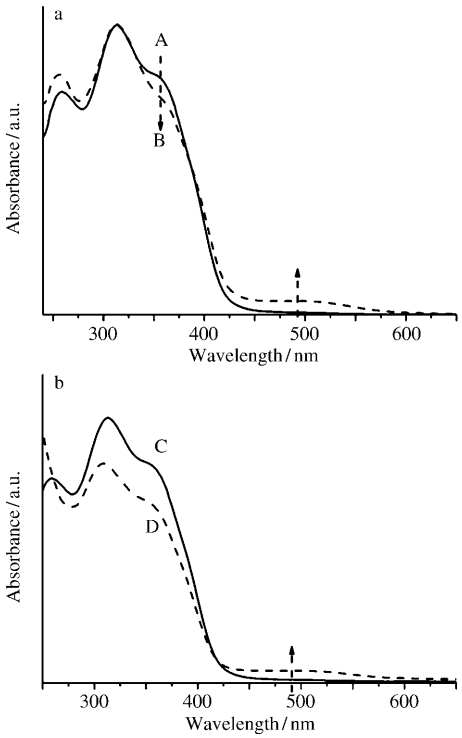

Figure 3. UV/Vis spectra of 3.8×10^{-5} M solutions of a) HCP-*star*-PEG (A) and HCP-*star*-PEG with 2 μL TFA (B) and b) HCP-*star*-PEG (C) and HCP-*star*-PEG with 2 mg $SnCl_2$ (D) in chloroform.

312 nm are attributed to π–π* excitations of the 3,6-carbazole unit and the shoulder peak at 355 nm is related to both the phenyleneethylene and imine moieties.[12] After the addition of trifluoroacetic acid (TFA), the absorption peak at 355 nm decreases and is redshifted to 490 nm. At the same time, the solution color changes from light-green to red, as shown in the Supporting Information. The shoulder peak at 363 nm arises from the absorption of phenyleneethylene. Note that the change in the optical properties of HCP-*star*-PEG in chloroform solution is reversed when triethylamine is added to neutralize the proton.

It is well known that the imine linkage is not coplanar with the neighboring carbazolylene ring because of the conjugation between the imine nitrogen lone-pair electrons and the π electrons in the carbazolylene ring. For HCP-*star*-PEG, the addition of acid leads to protonation of the imine group in the acylhydrazone bond, which enhances the planarity of the imine and carbazolylene ring.[13] Therefore the UV/Vis absorption of the imine group is redshifted to 490 nm, resulting in a change in the color of the solution. Owing to the amplification effect of the conjugated polymer[14] and plenty of acylhydrazone bonds in the hyperbranched structure, the optical properties of HCP-*star*-PEG in chloroform solution are very sensitive to acid.

Compared with the ^{1}H NMR spectrum of HCP-*star*-PEG, the proton peak arising from C*H*=N at $\delta = 9.4$ ppm disappears when trifluoroacetic acid is added to a [D]chloroform solution of the star polymer (Figure S5). Protonation of the imine group increases the efficient conjugated length of HCP-*star*-PEG and therefore the proton resonance of C*H*=N shifts upfield and overlaps with the aromatic ring signals.

To further confirm the influence of imine protonation on the optical properties, the HCP-*star*-PEG was also complexed with the Lewis acid $SnCl_2$. Figure 3b shows that the high absorption at 490 nm also appears after the addition of $SnCl_2$ and the color of the HCP-*star*-PEG solution changes from light-green to red (see the Supporting Information). This phenomenon indicates the coordination of Sn^{II} ions with the nitrogen atom of the imine linkage.[15]

Controlling the optical properties of the star copolymer through self-assembly: PEG can be dissolved both in chloroform and acetonitrile, whereas HCP is only soluble in chloroform. Thus, self-assembly only occurs when HCP-*star*-PEG is dissolved in acetonitrile or acetonitrile/chloroform cosolvent.

^{1}H NMR spectroscopy is a useful tool for studying the self-assembly process of amphiphilic hyperbranched copolymers.[16] Figure 4 shows the ^{1}H NMR spectra of HCP-*star*-PEG dissolved in $CDCl_3$ and CD_3CN, respectively. In both solvents, the peaks of OCH_2CH_2O in PEG ($\delta = 3.4$–3.9 ppm) are at the same position and are used as internal standards. Compared with in $CDCl_3$, in CD_3CN the aromatic proton peaks decrease dramatically and the acylhydrazone signal weakens. This NMR result demonstrates that the HCP-*star*-PEG molecules adopt a stretched conformation in chloroform solvent, whereas the collapsed HCPs are shielded by PEG arms in acetonitrile. In other words, the HCP core and acylhydrazone bonds are wrapped in the interior of the micelles by PEG arms and the micelles adopt core–shell structures.

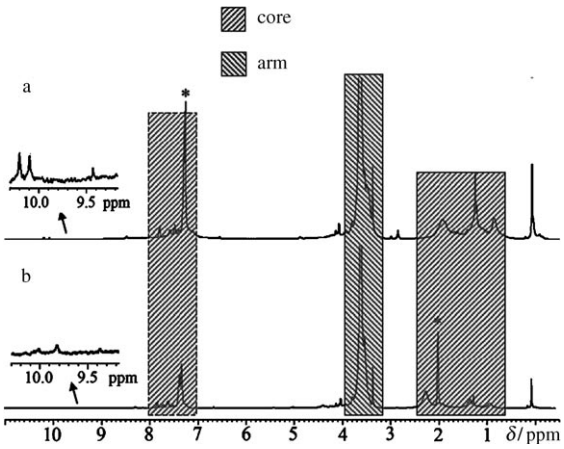

Figure 4. ^{1}H NMR spectra of HCP-*star*-PEG in a) $CDCl_3$, and b) CD_3CN (400 MHz, 20 °C; the solvent peak is marked with an asterisk).

Dynamic light scattering studies were carried out to investigate the hydrodynamic properties and self-assembly behavior of HCP-*star*-PEG in mixed solvents with different amounts of acetonitrile. In Figure 5a, the peak arising from HCP-*star*-PEG represents the unassociated unimolecule in chloroform with $D_h \approx 4$ nm. On addition of acetonitrile, the size of the particle increases to ~63 nm in pure acetonitrile.

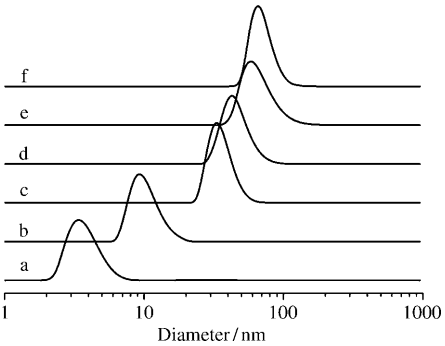

Figure 5. Typical number-weighted DLS plots of a HCP-*star*-PEG solution in mixed solutions of chloroform and acetonitrile. The content of acetonitrile is as follows: a) 0, b) 20, c) 40, d) 60, e) 80, and f) 100 %.

This result indicates that the HCP core of HCP-*star*-PEG collapses and aggregates to form core–shell micelles. When the content of acetonitrile is small, the HCP-*star*-PEG forms small micelles, as shown in Figure 5b. As acetonitrile increases, the HCP core further collapses and aggregates. Simultaneously, the secondary aggregation of micelles occurs through intermicellar interactions such as hydrogen bonds and van der Waals interactions, thus the micelles of HCP-*star*-PEG increase in size.[16a,17]

To confirm the DLS results, the size and morphology of HCP-*star*-PEG dissolved in mixed solvents were further investigated by TEM measurements. Figure 6a shows that there are few particles of HCP-*star*-PEG in chloroform. This indicates that it is difficult for the stretched molecular conformation to aggregate into micelles. With increasing acetonitrile content, the size of the micelles also increases. In Figure 6b–e, HCP-*star*-PEG forms micellar structures with average diameters of ~8, ~25, ~38, and ~44 nm, respectively, which are smaller than those determined by DLS. In general, the sizes determined by TEM are smaller than those determined by DLS. This is reasonable because TEM and DLS show a different morphology in the solid and swollen states, respectively. For HCP-*star*-PEG assembled in pure acetonitrile, the majority of the micelles are approximately 60 nm in diameter with some network-like aggregations, as shown in Figure 6f. It is considered that the intermolecular interactions between long PEG chains lead to network clusters when a solution of HCP-*star*-PEG dries on the substrate.[18]

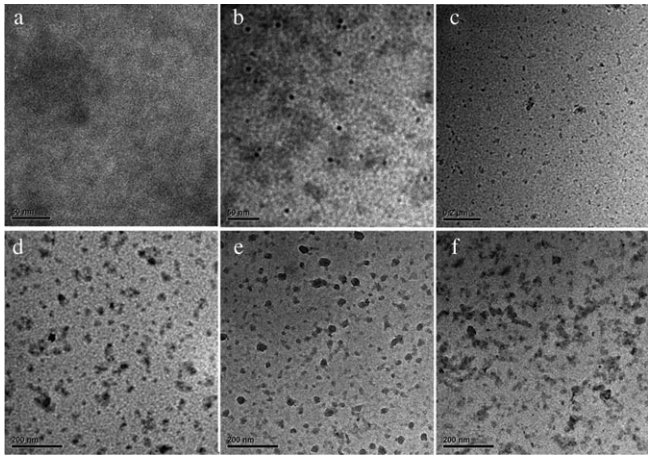

Figure 6. TEM photographs of HCP-*star*-PEG micelles in mixed solutions of chloroform and acetonitrile, the content of acetonitrile is as follows: a) 0, b) 20, c) 40, d) 60, e) 80, and f) 100 %. The scale bars represent 50 nm for a and b, and 200 nm for c–f.

Owing to the self-assembly of HCP-*star*-PEG to form core–shell micelles on addition of acetonitrile, the optical properties of HCP-*star*-PEG can readily be controlled. Figure 7a shows the UV/Vis spectra of HCP-*star*-PEG in chloroform/acetonitrile solution in the presence of TFA. Compared with the spectrum of HCP-*star*-PEG in pure chloroform solution, the absorption peak at 490 nm becomes less intense with increasing addition of acetonitrile. Because acetonitrile is a poor solvent of HCP, the addition of acetonitrile induces the collapse and aggregation of the HCP core, which protects the imine group from protonation. Consequently, the absorption at 490 nm is reduced and the color of HCP-*star*-PEG in the mixed solvent changes from red to light-green (see the Supporting Information). As increasing amounts of acetonitrile are added, the color of the solution fades.

Figure 7b shows the experimental plot of the absorbance at 490 nm as a function of acetonitrile content in HCP-*star*-PEG mixed solution. The UV/Vis absorption at 490 nm decreases very rapidly on increasing the acetonitrile content below 40 %. Above this critical point, the decrease of ab-

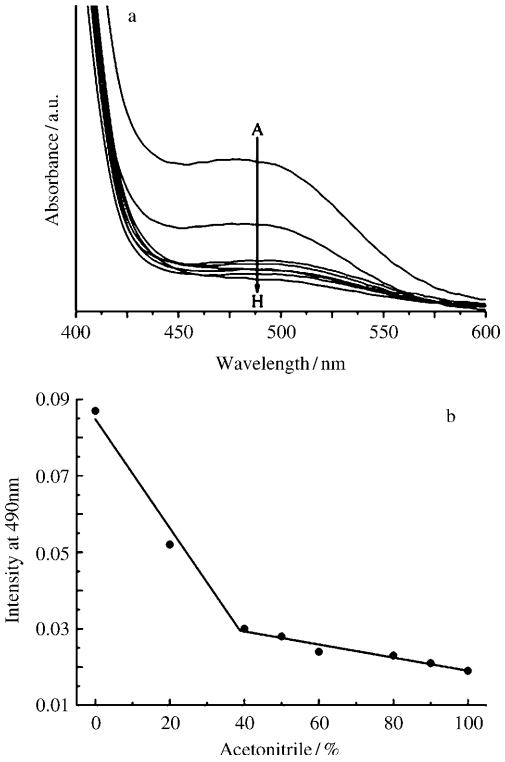

Figure 7. a) UV/Vis spectra at a concentration of 3.8×10^{-5} M of HCP-*star*-PEG in a mixed solution of chloroform and acetonitrile with TFA. The content of acetonitrile is as follows: A) 0, B) 20, C) 40, D) 50, E) 60, F) 80, G) 90, and H) 100 %. b) Absorbance at 490 nm as a function of added acetonitrile content in a chloroform solution of HCP-*star*-PEG.

sorbance becomes much slower. This indicates that the HCP-*star*-PEG assembles rapidly to give core–shell micelles on addition of acetonitrile to the solution. At the beginning, most of the imine bonds are isolated by the collapse and aggregation of the HCP core, leading to a sharp decline in the absorbance at 490 nm. However, as the acetonitrile content exceeds the critical point, further collapse of HCP core becomes difficult due to the rigidity of the backbone and steric hindrance. At the same time, secondary aggregation of the micelles occurs, but this does not isolate the imine bond from the proton very effectively. Thus, the intensity of the UV/Vis absorption decreases slowly and the color of the HCP-*star*-PEG solution changes only slightly. The proposed self-assembly model of HCP-*star*-PEG and its influence on the optical properties are illustrated in Scheme 2.

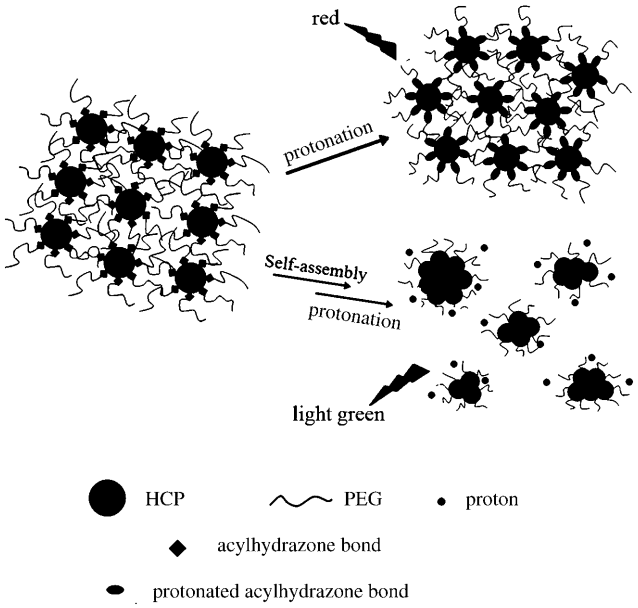

Scheme 2. Illustration of the control of the optical properties of HCP-*star*-PEG by self-assembly.

Conclusion

A facile and efficient method for controlling the optical properties of a star copolymer with a hyperbranched conjugated core (HCP-*star*-PEG) has been developed through self-assembly. The hyperbranched conjugated polymer (HCP) was synthesized successfully by an A_2+B_3-type Wittig coupling reaction and many linear PEGs were connected to the HCP through acylhydrazone bonds. The structures of HCP and HCP-*star*-PEG were characterized by ^{1}H NMR and FTIR spectroscopy. The degree of branching (DB) of HCP and the grafting ratio (g) of HCP-*star*-PEG were determined by ^{1}H NMR spectroscopy, with values of 0.77 and 0.91, respectively, obtained. Both the HCP and HCP-*star*-PEG exhibit good thermal and solubility properties. The optical properties of HCP-*star*-PEG in solution changed on addition of trifluoroacetic acid as well as $SnCl_2$, which demonstrates the complexation of the acid/metal ion and imine bond in acylhydrazone. Core–shell micelles were formed by self-assembly on addition of acetonitrile to HCP-*star*-PEG in chloroform solution. DLS and TEM experiments showed that the size of HCP-*star*-PEG micelles increased with acetonitrile content in a mixed solvent. The self-assembly of HCP-*star*-PEG prevented the protonation of the imine bond, which affected the optical properties of HCP-*star*-PEG greatly. Such control of the optical properties of the star copolymer by self-assembly may lead to new applications of conjugated polymers.

Experimental Section

Materials: Carbazole (98%, Alfa), mesitylene (98%, Alfa), 1-bromohexane (98%, Aldrich), poly(ethylene glycol) monomethyl ether (Fluka, $M_n=2000$), and potassium *tert*-butanolate (98%, Aldrich) were used without further purification. *N*-Bromosuccinimide (A.R.), triphenylphosphine (A.R.), benzoyl peroxide (A.R.), ethyl bromoacetate (A.R.), and hydrazine hydrate (85%) were purchased from Shanghai Chemical Reagent Co. and used as received. Phosphorus oxychloride, *N*,*N*-dimethylformamide (DMF), toluene, chloroform, and dichloromethane were heated at reflux with CaH_2, and then distilled prior to use. Tetrahydrofuran (THF) was heated at reflux over sodium wires and benzophenone until anhydride and then distilled to use immediately. Ethanol was heated at reflux with magnesium powder for several hours and catalyzed with iodine, then distilled to use. The other chemical reagents were purchased from domestic suppliers and used as received.

Synthesis of *N*-(*n*-hexyl)carbazole (1): The compound was synthesized by the reaction of carbazole and 1-bromohexane. 1-Bromohexane (3.30 g, 20 mmol) was added dropwise to a mixture of carbazole (3.25 g, 10 mmol) and potassium hydroxide (2.96 g, 52.8 mmol) in DMF (40 mL) and then allowed to react for 1 day at room temperature. The solution was poured into water to form a precipitate which was filtered. The precipitate thus obtained was dissolved in chloroform, washed with water three times, and dried with anhydrous magnesium sulfate. After evaporating the solvent, the residue was recrystallized from *n*-hexane. Yield: 80%. ^{1}H NMR (400 MHz, $CDCl_3$, 20°C): $\delta=0.87$ (t, $J=7.043$ Hz, 3H; CH_3), 1.26–1.43 (m, 6H; $CH_3C_3H_6$), 1.87 (m, 2H; NCH_2CH_2), 4.30 (t, $J=7.043$ Hz, 2H; NCH_2), 7.22 (t, $J=7.825$ Hz, 2H, Ar-H), 7.40–7.48 (m, 4H; Ar-H), 8.09 ppm (d, $J=7.825$ Hz, 2H; Ar-H); ^{13}C NMR (400 MHz, $CDCl_3$, 20°C): $\delta=14.63$ (CH_3), 23.11 (CH_3CH_2), 27.49 (CH_2CH_2), 29.44 (CH_2CH_2), 32.13 (CH_2CH_2), 43.44 (NCH_2), 109.18 (Ar-C), 119.23 (Ar-C), 120.86 (Ar-C), 123.34 (Ar-C), 126.09 (Ar-C), 140.94 ppm (Ar-C); IR (KBr): $\tilde{\nu}=3051$, 2955, 2923, 2869, 2856, 1628, 1594, 1487, 1453, 1376, 1327, 1241, 1217, 1192, 1153, 1128 cm^{-1}.

Synthesis of *N*-(*n*-hexyl)-3,6-diformylcarbazole (2): Phosphoryl chloride (25 mL, 0.27 mol) was added dropwise to *N*,*N*-dimethylformamide (DMF, 35 mL, 0.45 mol) for 1 h at 0°C. The mixture was stirred and then *N*-(*n*-hexyl)carbazole (4.00 g, 16 mmol) in dichloromethane (20 mL) was added over 2 h at room temperature. After standing for 48 h at 90°C, the mixture was poured into ice–water (300 mL), stirred overnight, and neutralized with sodium hydroxide. The solution was extracted three times with chloroform and dried with anhydrous magnesium sulfate. The solvent was removed under reduced pressure. The residue was purified by silica gel column chromatography (eluent: ethyl acetate/petroleum ether=1:2). Yield: 72%. ^{1}H NMR (400 MHz, $CDCl_3$, 20°C): $\delta=0.87$ (t, $J=7.043$ Hz, 3H; CH_3), 1.25–1.42 (m, 6H; $CH_3C_3H_6$), 1.92 (m, 2H; NCH_2CH_2), 4.39 (t, $J=7.043$ Hz, 2H; NCH_2), 7.55 (d, $J=8.608$ Hz, 2H; Ar-H), 8.08 (d, $J=8.608$ Hz, 2H; Ar-H), 8.68 (s, 2H; Ar-H), 10.14 ppm (s, 2H; CHO); ^{13}C NMR (400 MHz, $CDCl_3$, 20°C): $\delta=14.19$ (CH_3), 22.70 (CH_3CH_2), 27.02 (CH_3CH_2), 29.06 (CH_3CH_2), 31.63 (CH_3CH_2), 43.89 (NCH_2), 110.00 (Ar-C), 123.17 (Ar-C), 124.20 (Ar-C), 127.99 (Ar-C), 129.58 (Ar-C), 144.83 (Ar-C), 191.60 ppm (CHO); IR (KBr): $\tilde{\nu}=2960$, 2929, 2862, 2725, 1686, 1630, 1597, 1574, 1488, 1465, 1438, 1385, 1352, 1306, 1290, 1243, 1210, 1124 cm^{-1}.

Synthesis of 1,3,5-tris(bromomethyl)benzene (3): The chemical compound was synthesized according to a modification of a previously reported method.[12a] A mixture containing mesitylene (5 mL, 36 mmol), *N*-bromosuccinimide (19.49 g, 109.5 mmol), and benzoyl peroxide (0.1986 g, 0.82 mmol) in benzene (150 mL) was heated to initiate the reaction at a reflux temperature of 95±1 °C. Although the reaction was strongly exothermic to ensure the solution boils, the self-reflux time of this system was kept for only 0.5 h. To ensure the bromination reaction went to completion, the solution was reheated at reflux for several hours. After filtering, the filtrate was washed with water and dried with anhydrous magnesium sulfate. The needle crystals were achieved as the solution was concentrated, with further recrystallization in a mixture of ethanol and hexane (1:1). Yield: 88%. ^{1}H NMR (400 MHz, $CDCl_3$, 20 °C): δ = 4.455 (s, 6H; CH_2Br), 7.353 ppm (s, 3H; Ar-H); ^{13}C NMR (400 MHz, $CDCl_3$, 20 °C): δ = 32.61 (CH_2Br), 129.87 (Ar-C), 139.28 ppm (Ar-C); IR (KBr): $\tilde{\nu}$ = 3026, 2971, 2921, 2850, 1803, 1713, 1611, 1458, 1439, 1217, 1170, 1123, 986, 900, 861, 705, 591, 560 cm^{-1}.

Synthesis of 1,3,5-bis[(triphenylphosphonio)methyl]benzene tribromide (4): A solution of 1,3,5-tris(bromomethyl)benzene (1.45 g, 4.07 mmol), triphenylphosphine (3.59 g, 13.67 mmol), and ethanol (60 mL) was heated at reflux for 24 h under nitrogen. The solution was poured into THF (200 mL) after being cooled to room temperature and concentrated to 20 mL. The white precipitate was filtered and thoroughly dried under vacuum. Yield: 81%. ^{1}H NMR (400 MHz, [D$_6$]DMSO, 20 °C): δ = 4.88 (d, J = 7.825 Hz, 6H; CH_2Br), 6.68 (s, 3H; Ar-H), 7.44–7.49 (m, 18H; Ar-H), 7.61–7.66 (m, 18H; Ar-H), 7.85 ppm (t, J = 7.043 Hz, 9H; Ar-H); ^{13}C NMR (400 MHz, [D$_6$]DMSO, 20 °C) δ = 117.94 (CH_2Br), 118.79 (Ar-C), 130.83 (Ar-C), 130.95 (Ar-C), 134.31 (Ar-C), 134.40 (Ar-C), 135.77 ppm (Ar-C); IR (KBr): $\tilde{\nu}$ = 3054, 3007, 2858, 2784, 1592, 1486, 1439, 1408, 1322, 1119, 1002, 974, 751, 724, 697, 517 cm^{-1}.

Synthesis of poly(ethylene glycol) monomethyl ether with ethyl acetate terminals (PEG-$CH_2COOC_2H_5$, 5): PEG monomethyl ether (M_n = 2000, 10.40 g, 5.2 mmol) was fully dissolved in toluene (100 mL) and potassium *tert*-butoxide (2.05 g, 18 mmol) dissolved in *tert*-butyl alcohol (30 mL) was added. Then ethyl bromoacetate (3.2 mL, 28 mmol) was added slowly over a period of 30 min. The solution was stirred at room temperature for 24 h, filtered, concentrated with dichloromethane, and precipitated in diethyl ether three times to obtain a white solid product. The precipitate was dried under a vacuum at room temperature. Yield: 92%. ^{1}H NMR (400 MHz, [D$_6$]DMSO, 20 °C): δ = 1.18 (t, J = 7.043 Hz, 3H; CH_3), 3.22 (s, 3H; OCH_3), 3.31–3.66 (m, 180H; OCH_2CH_2), 4.22 (m, 2H; OCH_2CH_2OCO), 4.70 ppm (s, 2H; $OCOOCH_2$); ^{13}C NMR (400 MHz, [D$_6$]DMSO, 20 °C): δ = 14.62 (CH_3), 61.29 (OCH_3), 68.06–71.95 (OCH_2CH_2), 170.52 ppm (C=O); IR (KBr): $\tilde{\nu}$ = 2286, 1756, 1471, 1365, 1346, 1283, 1240, 1115, 962, 841 cm^{-1}.

Synthesis of poly(ethylene glycol) monomethyl ether with acylhydrazine terminals (PEG-$CH_2CONHNH_2$, 6): PEG-$CH_2COOC_2H_5$ (**5**; 10.00 g, 4.8 mmol) was dissolved in methanol (100 mL) and a mixture of hydrazine hydrate (30 mL) and methanol (40 mL) was added to the solution dropwise. After reaction for 24 h at room temperature, the solution was filtered. Then most of the methanol solvent was removed under reduced pressure. The concentrated solution was extracted with dichloromethane, dried with anhydrous magnesium sulfate and precipitated with anhydrous diethyl ether. The white precipitate was dried under a vacuum at room temperature. Yield: 90%. ^{1}H NMR (400 MHz, [D$_6$]DMSO, 20 °C): δ = 3.22 (s, 3H; OCH_3), 3.30–3.68 (m, 180H; OCH_2CH_2), 3.87 (s, 2H; OCH_2CH_2OCO), 8.87 ppm (s, 1H; $CONHNH_2$); ^{13}C NMR (400 MHz, [D$_6$]DMSO, 20 °C): δ = 60.89 (OCH_3), 70.27–73.00 (OCH_2CH_2), 168.77 ppm (C=O); IR (KBr): $\tilde{\nu}$ = 3425, 3323, 2889, 1676, 1471, 1365, 1346, 1279, 1240, 1111, 959, 841 cm^{-1}.

Synthesis of the hyperbranched conjugated polymer (HCP, 7): A solution of sodium (0.083 g, 3.6 mmol) in anhydrous ethanol (5 mL) was added dropwise at ambient temperature under nitrogen to a mixture of *N*-(*n*-hexyl)-3,6-diformylcarbazole (**2**; 0.491 g, 1.6 mmol) and the phosphonium salt **4** (0.915 g, 0.8 mmol) in anhydrous ethanol and dry chloroform (1:2, 30 mL). The mixture was stirred at room temperature overnight. The polymerization was quenched by adding dilute hydrochloric acid (2% in water, 5 mL) and stirred for a few minutes. The resultant was dissolved in chloroform and filtered. The filtrate was concentrated under reduced pressure and added slowly to methanol at room temperature to form a precipitate. Reprecipitation was performed three times and a bright-yellow polymer was obtained after drying under vacuum at 40 °C. Yield: 71%. ^{1}H NMR (400 MHz, $CDCl_3$, 20 °C): δ = 0.42–0.98 (br, CH_3), 0.98–1.45 (br, CH_2CH_3), 1.45–2.45 (br, NCH_2CH_2), 3.60–4.65 (br, NCH_2), 5.78–8.85 (m, Ar-H), 9.62–10.28 ppm (br, CHO); ^{13}C NMR (400 MHz, $CDCl_3$, 20 °C): δ = 14.25 (CH_3), 22.75 (CH_3CH_2), 27.10 (CH_2CH_2), 29.12 (CH_2CH_2), 29.96 (CH_2CH_2), 31.71 (NCH_2CH_2), 43.42 (NCH_2), 109.19 (Ar-C), 118.96–131.13 (Ar-C), 134.60 (Ar-C), 138.27–140.62 (Ar-C), 144.38 (Ar-C), 191.86 ppm (CHO); IR (KBr): $\tilde{\nu}$ = 3011, 2949, 2923, 2851, 2719, 1684, 1623, 1587, 1485, 1382, 1346, 1238, 1190, 1153, 1129, 955, 879, 798 cm^{-1}.

Synthesis of a star copolymer with a hyperbranched conjugated polymer core and many linear PEG arms (HCP-*star*-PEG): A solution containing the hyperbranched conjugated polymer and a certain amount of PEG-$CH_2CONHNH_2$ (**6**) in anhydrous THF was allowed to react under nitrogen at 60 °C for 24 h. After cooling to room temperature, the solution was concentrated and precipitated three times with anhydrous methanol. The precipitate was dissolved in chloroform and washed with deionized water several times and dried with anhydrous magnesium sulfate. The product was obtained by removing the solvent under reduced pressure and drying in a vacuum at room temperature. Yield: 62%. ^{1}H NMR (400 MHz, $CDCl_3$, 20 °C): δ = 0.45–0.98 (br, CH_3), 0.98–1.45 (br, CH_2CH_3), 1.45–2.50 (br, NCH_2CH_2), 3.37 (br, OCH_3), 3.38–4.98 (m, CH_2CH_2O), 4.05–4.42 (br, NCH_2), 6.25–8.85 (m, Ar-H), 9.40 (br, ArCH=N), 10.1 (br, CHO), 10.2 ppm (br, NHCO); ^{13}C NMR (400 MHz, $CDCl_3$, 20 °C): δ = 14.21 (CH_3), 22.66 (CH_3CH_2), 27.03 (CH_2CH_2), 29.11 (CH_2CH_2), 29.85 (CH_2CH_2), 31.67 (NCH_2CH_2), 43.50 (NCH_2), 59.22, 61.81 (OCH_3), 69.51–72.81 (OCH_2CH_2), 109.43 (Ar-C), 123.12 (Ar-C), 128.77 (Ar-C), 132.23–134.27 (Ar-C), 138.29–140.74 (Ar-C), 144.27 (Ar-C), 171.86 (Ar-CH=N), 191.86 ppm (CHO); IR (KBr): $\tilde{\nu}$ = 3433, 2881, 1684, 1624, 1594, 1485, 1467, 1386, 1355, 1343, 1280, 1241, 1111, 964, 843 cm^{-1}.

Self-assembly of the star copolymer HCP-*star*-PEG in mixed solvents: HCP-*star*-PEG (20 mg) dissolved in chloroform (4 mL) was stirred uniformly before use. Under gentle stirring, different amounts of acetonitrile were added dropwise to the chloroform solution to give certain content in solution. The final concentration of HCP-*star*-PEG in the resultant solution was set to 1 mg mL^{-1} (3.8×10^{-5} M). All procedures were performed at room temperature.

NMR spectroscopy: NMR spectra were recorded on a Varian Mercury Plus 400 MHz spectrometer with deuteriated dimethyl sulfoxide ([D$_6$]DMSO), deuteriated chloroform ($CDCl_3$), deuteriated dichloromethane (CD_2Cl_2) and deuteriated acetonitrile (CD_3CN) as solvents at 20 °C. Tetramethylsilane (TMS) was used as the internal reference.

FTIR spectroscopy: FTIR spectra were recorded on a Paragon 1000 instrument by using the KBr sample holder method.

Gel permeation chromatography (GPC): The number-average molecular weights (M_n) and the polydispersity (M_w/M_n) indices were determined by gel permeation chromatography/multi-angle laser light-scattering (GPC-MALLS). The gel permeation chromatography system consisted of a Waters degasser, a Waters 515 HPLC pump, a 717 automatic sample injector, a Wyatt Optilab DSP differential refractometer detector, and a Wyatt miniDAWN multi-angle laser light-scattering detector. Three chromatographic columns (styragel HR3, HR4, and HR5) were used in series. THF was used as the mobile phase at a flow rate of 1 mL min^{-1} at 30 °C. The refractive index increment dn/dc was determined with a Wyatt Optilab DSP differential refractometer at 690 nm. Data analysis was performed with Astra software (Wyatt Technology).[19]

Thermal gravimetric analysis (TGA): TGA measurements were performed on a Perkin–Elmer TGA-7 thermogravimetric analyzer to investigate the thermal stability of all samples in a nitrogen atmosphere from ambient temperature to 800 °C at 20 °C min^{-1}.

Transmission electron microscopy (TEM): TEM studies were performed with a JEOL JEM-100CX-II instrument at a voltage of 200 kV. Samples were prepared by drop-casting micelle solutions onto carbon-coated

copper grids and then air-drying at room temperature before measurement.

Dynamic light scattering (DLS): DLS measurements were performed with a Malvern Zetasizer Nano S apparatus (Malvern Instruments Ltd) equipped with a 4.0 mW He–Ne laser operating at $\lambda = 633$ nm. All samples were measured at room temperature and a scattering angle of 173°.

UV/Vis spectrophotometry: UV/Vis spectra were performed with a Thermo Evolution 300 UV/Vis spectrophotometer in the range of 200–800 nm.

Acknowledgements

This work was sponsored by the National Natural Science Foundation of China (50773037, 50633010, and 20974062), the National Basic Research Program (2009CB930400), the Fok Ying Tung Education Foundation (111048), the Shuguang Program (08SG14), the Shanghai Rising-Star Program (08A14037), and the Shanghai Leading Academic Discipline Project (B202).

[1] a) H. Ringsdorf, J. Simon, *Nature* **1994**, *371*, 284–284; b) G. M. Whitesides, B. Grzybowski, *Science* **2002**, *295*, 2418–2421; c) L. Zhang, A. Eisenberg, *Science* **1995**, *268*, 1728–1731; d) Y. Y. Won, H. T. Davis, F. S. Bates, *Science* **1999**, *283*, 960–963; e) R. Oda, I. Huc, M. Schmutz, S. J. Candau, F. C. MacKintosh, *Nature* **1999**, *399*, 566–569; f) S. I. Stupp, V. LeBonheur, K. Walker, L. S. Li, K. E. Huggins, M. Keser, A. Amstutz, *Science* **1997**, *276*, 384–389; g) D. Y. Yan, Y. F. Zhou, J. Hou, *Science* **2004**, *303*, 65–67.

[2] a) F. J. M. Hoeben, L. M. Herz, C. Daniel, P. Jonkheijm, A. Schenning, C. Silva, S. C. J. Meskers, D. Beljonne, R. T. Phillips, R. H. Friend, E. W. Meijer, *Angew. Chem.* **2004**, *116*, 2010–2013; *Angew. Chem. Int. Ed.* **2004**, *43*, 1976–1979; b) B. K. An, D. S. Lee, J. S. Lee, Y. S. Park, H. S. Song, S. Y. Park, *J. Am. Chem. Soc.* **2004**, *126*, 10232–10233; c) K. Balakrishnan, A. Datar, T. Naddo, J. L. Huang, R. Oitker, M. Yen, J. C. Zhao, L. Zang, *J. Am. Chem. Soc.* **2006**, *128*, 7390–7398; d) J. Y. Park, N. Koenen, M. Forster, R. Ponnapati, U. Scherf, R. Advincula, *Macromolecules* **2008**, *41*, 6169–6175.

[3] a) J. Bae, J. H. Choi, Y. S. Yoo, N. K. Oh, B. S. Kim, M. Lee, *J. Am. Chem. Soc.* **2005**, *127*, 9668–9669; b) M. M. S. Abdel-Mottaleb, G. Gotz, P. Kilickiran, P. Bauerle, E. Mena-Osteritz, *Langmuir* **2006**, *22*, 1443–1448.

[4] a) A. Heyen, C. C. Buron, Q. Tianshi, R. Bauer, A. M. Jonas, K. Müllen, F. C. De Schryver, S. De Feyter, *Small* **2008**, *4*, 1160–1167; b) X. L. Feng, Y. Y. Liang, L. J. Zhi, A. Thomas, D. Q. Wu, I. Lieberwirth, U. Kolb, K. Müllen, *Adv. Funct. Mater.* **2009**, *19*, 2125–2129.

[5] a) P. Leclère, M. Surin, P. Viville, R. Lazzaroni, A. F. M. Kilbinger, O. Henze, W. J. Feast, M. Cavallini, F. Biscarini, A. Schenning, E. W. Meijer, *Chem. Mater.* **2004**, *16*, 4452–4466; b) Y. F. Tao, B. W. Ma, R. A. Segalman, *Macromolecules* **2008**, *41*, 7152–7159; c) S. R. Diegelmann, J. M. Gorham, J. D. Tovar, *J. Am. Chem. Soc.* **2008**, *130*, 13840–13841; d) K. Li, H. Guo, Z. Q. Liang, P. Thiyagarajan, Q. Wang, *J. Polym. Sci. Polym. Chem. Ed.* **2005**, *43*, 6007–6019; e) C. H. Lin, Y. C. Tung, J. Ruokolainen, R. Mezzenga, W. C. Chen, *Macromolecules* **2008**, *41*, 8759–8769; f) L. Rubatat, X. X. Kong, S. A. Jenekhe, J. Ruokolainen, M. Hojeij, R. Mezzenga, *Macromolecules* **2008**, *41*, 1846–1852; g) F. K. Wang, G. C. Bazan, *J. Am. Chem. Soc.* **2006**, *128*, 15786–15792; h) A. de Cuendias, E. Ibarboure, S. Lecommandoux, E. Cloutet, H. Cramail, *J. Polym. Sci. Polym. Chem. Ed.* **2008**, *46*, 4602–4616; i) X. Xiao, Y. G. Wu, M. H. Sun, J. J. Zhou, Z. S. Bo, L. Li, C. M. Chan, *J. Polym. Sci. Polym. Chem. Ed.* **2008**, *46*, 574–584.

[6] a) J. F. Hulvat, M. Sofos, K. Tajima, S. I. Stupp, *J. Am. Chem. Soc.* **2005**, *127*, 366–372; b) A. Schenning, A. F. M. Kilbinger, F. Biscarini, M. Cavallini, H. J. Cooper, P. J. Derrick, W. J. Feast, R. Lazzaroni, P. Leclere, L. A. McDonell, E. W. Meijer, S. C. J. Meskers, *J. Am. Chem. Soc.* **2002**, *124*, 1269–1275; c) H. C. Lin, K. W. Lee, C. M. Tsai, K. H. Wei, *Macromolecules* **2006**, *39*, 3808–3816; d) Y. F. Tao, B. McCulloch, S. Kim, R. A. Segalman, *Soft Matter* **2009**, *5*, 4219–4230.

[7] H. Maeda, Y. Ito, Y. Haketa, N. Eifuku, E. Lee, M. Lee, T. Hashishin, K. Kaneko, *Chem. Eur. J.* **2009**, *15*, 3706–3719.

[8] a) X. M. Liu, T. T. Lin, J. C. Huang, X. T. Hao, K. S. Ong, C. B. He, *Macromolecules* **2005**, *38*, 4157–4168; b) Z. Ma, S. Lu, Q. L. Fan, C. Y. Qing, Y. Y. Wang, P. Wang, W. Huang, *Polymer* **2006**, *47*, 7382–7390; c) R. Wang, W. Z. Wang, G. Z. Yang, T. X. Liu, J. S. Yu, Y. D. Jiang, *J. Polym. Sci. Polym. Chem. Ed.* **2008**, *46*, 790–802; d) L. Ding, Z. S. Bo, Q. H. Chu, J. Li, L. M. Dai, Y. Pang, F. E. Karasz, M. E. Durstock, *Macromol. Chem. Phys.* **2006**, *207*, 870–878; e) J. Z. Liu, R. H. Zheng, Y. H. Tang, M. Haussler, J. W. Y. Lam, A. Qin, M. X. Ye, Y. N. Hong, P. Gao, B. Z. Tang, *Macromolecules* **2007**, *40*, 7473–7486; f) A. J. Qin, J. W. Y. Lam, C. K. W. Jim, L. Zhang, J. J. Yan, M. Haussler, J. Z. Liu, Y. Q. Dong, D. H. Liang, E. Q. Chen, G. C. Jia, B. Z. Tang, *Macromolecules* **2008**, *41*, 3808–3822; g) L. R. Tsai, Y. Chen, *J. Polym. Sci. Polym. Chem. Ed.* **2007**, *45*, 5541–5551.

[9] Q. Q. He, H. M. Huang, F. L. Bai, Y. Cao, *Macromol. Rapid Commun.* **2006**, *27*, 302–305.

[10] a) Y. H. Kim, O. W. Webster, *Macromolecules* **1992**, *25*, 5561–5572; b) J. Z. Yao, D. Y. Son, *Organometallics* **1999**, *18*, 1736–1740; c) M. Jikei, M. Kakimoto, *Prog. Polym. Sci.* **2001**, *26*, 1233–1285; d) C. Gao, D. Yan, *Prog. Polym. Sci.* **2004**, *29*, 183–275; e) M. Häussler, R. H. Zheng, J. W. Y. Lam, H. Tong, H. C. Dong, B. Z. Tang, *J. Phys. Chem. B* **2004**, *108*, 10645–10650; f) Q. Zhu, J. L. Wu, C. L. Tu, Y. F. Shi, L. He, R. B. Wang, X. Y. Zhu, D. Y. Yan, *J. Phys. Chem. B* **2009**, *113*, 5777–5780.

[11] a) A. J. Qin, J. W. Y. Lam, H. C. Dong, W. X. Lu, C. K. W. Jim, Y. Q. Dong, M. Haussler, H. H. Y. Sung, I. D. Williams, G. K. L. Wong, B. Z. Tang, *Macromolecules* **2007**, *40*, 4879–4886; b) H. C. Dong, R. H. Zheng, J. W. Y. Lam, M. Haussler, A. J. Qin, B. Z. Tang, *Macromolecules* **2005**, *38*, 6382–6391.

[12] a) L. Jiuyan, L. Di, L. Yanqing, L. Chun-Sing, K. Hoi-Lun, L. Shuittong, *Chem. Mater.* **2005**, *17*, 1208–1212; b) R. Guan, Y. H. Xu, L. Ying, W. Yang, H. B. Wu, Q. L. Chen, Y. Cao, *J. Mater. Chem.* **2009**, *19*, 531–537; J. Q. Qu, M. Shiotsuki, N. Kobayashi, F. Sanda, T. Masuda, *Polymer* **2007**, *48*, 6481–6490.

[13] a) A. Iwan, D. Sek, J. Kasperczyk, *Macromolecules* **2005**, *38*, 4384–4392; b) B. Dufour, P. Rannou, D. Djurado, H. Janeczek, M. Zagorska, A. de Geyer, J. P. Travers, A. Pron, *Chem. Mater.* **2003**, *15*, 1587–1592; c) B. Pedras, E. Oliveira, H. Santos, L. Rodriguez, R. Crehuet, T. Aviles, J. L. Capelo, C. Lodeiro, *Inorg. Chim. Acta* **2009**, *362*, 2627–2635; d) D. Sek, A. Iwan, H. Janeczek, P. Rannou, A. Pron, *Thin Solid Films* **2004**, *453*, 362–366.

[14] S. W. Thomas, G. D. Joly, T. M. Swager, *Chem. Rev.* **2007**, *107*, 1339–1386.

[15] a) K. Yamamoto, M. Higuchi, S. Shiki, M. Tsuruta, H. Chiba, *Nature* **2002**, *415*, 509–511; b) M. Higuchi, M. Tsuruta, H. Chiba, S. Shiki, K. Yamamoto, *J. Am. Chem. Soc.* **2003**, *125*, 9988–9997.

[16] a) Y. Y. Mai, Y. F. Zhou, D. Y. Yan, *Macromolecules* **2005**, *38*, 8679–8686; b) H. Y. Hong, Y. Y. Mai, Y. F. Zhou, D. Y. Yan, Y. Chen, *J. Polym. Sci. Polym. Chem. Ed.* **2008**, *46*, 668–681.

[17] H. Y. Hong, Y. Y. Mai, Y. F. Zhou, D. Y. Yan, J. Cui, *Macromol. Rapid Commun.* **2007**, *28*, 591–596.

[18] a) K. Y. Mya, X. Li, L. Chen, X. P. Ni, J. Li, C. B. He, *J. Phys. Chem. B* **2005**, *109*, 9455–9462; b) T. Song, S. Dai, K. C. Tam, S. Y. Lee, S. H. Goh, *Langmuir* **2003**, *19*, 4798–4803.

[19] Z. F. Jia, G. L. Li, Q. Zhu, D. Y. Yan, X. Y. Zhu, H. Chen, J. L. Wu, C. L. Tu, J. Sun, *Chem. Eur. J.* **2009**, *15*, 7593–7600.

Received: April 23, 2010
Published online: September 17, 2010

